AL54 - Model Predictive Control of Maintaining the Superheat of an Aluminium Smelting Cell during Power Modulation

Luning Ma[1], Choon-Jie Wong[2], Jie Bao[3], Maria Skyllas-Kazacos[4], Barry Welch[5], Nadia Ahli[6], Amal Aljasmi[7] and Mohamed Mahmoud[8]

1. PhD student
2. Postdoctoral Research fellow
3. Professor
4. Professor
5. Professor

School of Chemical Engineering, The University of New South Wales, Sydney, Australia

6. Manager, Technology Transfer Contracts
7. Area Engineer, Reduction Engineering
8. Manager, Centre of Excellence

Emirates Global Aluminium (EGA), United Arab Emirates

Corresponding author: j.bao@unsw.edu.au

Abstract

Superheat is a crucial indicator of the thermal balance in the aluminium smelting process. Maintaining the superheat within a narrow range ensures the productivity and energy efficiency. Large fluctuations in superheat can result in undesirable effects such as increased back reactions, sludge formation and reduced current efficiency. Furthermore, during power modulation, the variable power input will affect cell thermal balance and increase the difficulty of cell operations. To reduce the variation of the superheat during power modulation, this paper develops a Model Predictive Control (MPC) approach to maintaining the superheat by manipulating the alumina feed and anode-cathode distance based on real-time temperature measurements or estimation. Through mathematical modelling and simulations, the mass and heat balance inside the cell is regulated during power modulation. This method provides an insight into superheat management for idle operation and power modulation.

Keywords: Aluminium electrolysis, Process control, Model predictive control.

1. Introduction

Controlling the aluminium smelting process is challenging due to its nonlinear characteristics, and coupled mass and thermal balance. Research in the literature mainly focuses on either the control of alumina concentration or the bath temperature and excess AlF_3 concentration [1-4]. Drengstig [2] mentioned the basic framework to control the bath temperature and excess AlF_3, and Kolås et. al. [3] adopted a PI control to control the bath temperature and excess AlF_3 by adjusting AlF_3 feed and ACD, whereas Shi [4] improved the alumina feeding control and used a state observer to estimate the alumina concentration. However, to control the process effectively, both mass balance and thermal balance should be managed simultaneously due to their coupling nature.

The superheat of an aluminium smelting cell is an important variable which can reflect the cell operation status. It is given by the difference between the bath temperature and the liquidus temperature. Controlling the superheat within a certain range is helpful for maintaining stable process conditions. If the superheat increases by 10 ^{o}C, the current efficiency will decrease by 1.2–1.5 % [5, 6]. Superheat is commonly regarded as the thermal driving force in the cell. As it provides the energy to dissolve alumina feed in the bath, a low superheat makes it difficult for alumina to dissolve [7]. On the other hand, increasing the superheat can lead to ledge melting,

while decreasing the superheat can cause ledge freezing, both of which can affect the chemical composition of the bath. The liquidus temperature is related to the bath composition, primarily the alumina concentration and the aluminium fluoride concentration, as their concentrations typically change more rapidly over time than others. Kolås [3] used a PID controller with anti-windup to calculate aluminium fluoride feed with assuming the aluminium fluoride consumption can be estimated. Drengstig [8] adopted an almost constant AlF_3 input to control the aluminium fluoride concentration. This input was determined through a simple mass balance calculation to ensure that the average addition matched the average consumption. However, controlling the aluminium fluoride concentration is still challenging as it is relatively easy to add but difficult to remove from the cell quickly. If an excessive amount of aluminium fluoride feed is introduced, it can have a long-term negative effect on the cell process. This may cause a significant decrease in the liquidus temperature, resulting in an increase of superheat and increasing the risk of the ledge completely melting. Regarding the alumina concentration, controlling the alumina feed is more convenient than controlling the aluminium fluoride feed since alumina is the primary material consumed in the production of aluminium. Additionally, an increase of 1 % alumina concentration can lead to a decrease in the liquidus temperature of approximately 5 °C [9]. Therefore, achieving effective control of the superheat requires proper management of both the bath temperature and the alumina concentration.

On the other hand, maintaining the superheat by simultaneously managing the bath temperature and alumina concentration plays a crucial role in power modulation. When the line current undergoes changes, rapid adjustment of both thermal balance and mass balance is necessary. Otherwise, failing to do so can lead to excessive superheat, increasing the risk of complete ledge melting, or insufficient superheat, causing excessive freezing of cryolite. In reference [10], the thermal response of power modulation events was demonstrated using a "lump parameter+" model. Eisma et. Al. [11] presented the cell performance of a TRIMET EPT-14 cell during a 24-hour period of a 20 kA reduction line (from 167 kA to 147 kA), and outlined the corresponding challenges during this process. In order to address the challenge of maintaining a stable process during power modulation, advanced algorithms should be considered. Model predictive control is an algorithm that can provide a powerful framework for controlling dynamic systems. By incorporating model-based predictions, optimization, and real-time decision-making while considering system constraints, MPC can effectively achieve desired objectives. Therefore, to address this challenge and maintain a stable process during power modulation, this paper adopts the MPC method.

The scope of this paper is to introduce a control scheme that maintains the superheat within a narrow range during power modulation in an aluminium smelting process by using MPC. Section 2 provides a concise system description and modelling of the aluminium smelting process. Section 3 outlines the controller design for MPC, while section 4 presents the simulation results.

2. System Description

The Hall-Héroult process is the only industrial method for producing aluminium. In this process, alumina is dissolved in molten cryolite at high temperature. When current is passed through the bath, aluminium ions migrate to the cathode, where they are reduced to form aluminium metal. Simultaneously, carbon dioxide or carbon monoxide is generated and released at the anode. The fundamental structure of an aluminium smelting cell is depicted in Figure 1. The overall electrochemical reaction, including reduction of alumina (forward reaction) and reoxidation of aluminium in the electrolyte is:

$$2\eta Al_2O_3 + 3C = 4\eta Al + 3(2\eta-1)CO_2 + 6(1-\eta)CO \quad (1)$$

where: η Fractional current efficiency, typically = 0.92-0.96.

Typically, the ratio of CO_2 to CO in the product gas is in the range of 5:1 to 10:1 [4]. This process model can be characterised by the following dynamics.

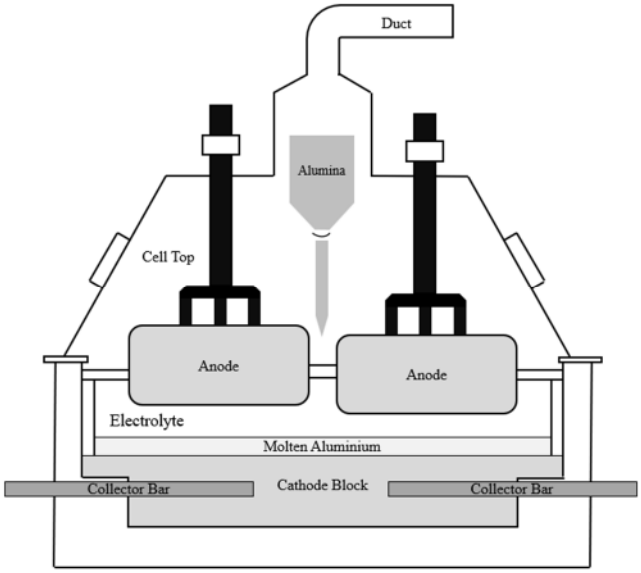

Figure 1. The basic structure of an aluminium smelting cell.

In terms of mass balance, the dissolution of alumina powder in cryolite is a complex process that involves factors such as heat transfer, initial alumina concentration, stirring speed and superheat [9]. Some of the alumina will sink into the bath and dissolve quickly, while some of it will float on the surface of the bath and dissolve slowly. In this paper, a simplified first-order model with considering two dissolution mechanisms is adopted as follows [12, 13]

$$\frac{dC_{Al_2O_3,fast}(t)}{dt} = -k_{fast} \times C_{Al_2O_3,fast}(t) + \frac{mass_{feed}(t) \times r}{mass_{bath}} \quad (2)$$

$$\frac{dC_{Al_2O_3,slow}(t)}{dt} = -k_{slow} \times C_{Al_2O_3,fast}(t) + \frac{mass_{feed}(t) \times (1-r)}{mass_{bath}} \quad (3)$$

where:

$C_{Al_2O_3,fast}$	Concentration of undissolved alumina which can dissolve into the bath quickly, %wt
$C_{Al_2O_3,slow}$	Concentration of undissolved alumina which can dissolve into the bath slowly, %wt
k_{fast}	Fast dissolution rate constant of undissolved alumina, s^{-1}
k_{slow}	Slow dissolution rate constant of undissolved alumina, s^{-1}
$mass_{feed}$	Mass of alumina being fed into the bath and, g/s
$mass_{bath}$	Mass of bath, g
r	Fraction of fast dissolving alumina in the alumina feed.

With the dynamics of fast and slow dissolving alumina, the equation for the dissolved alumina can be expressed as follows:

$$\frac{dC_{Al_2O_3,d}(t)}{dt} = (k_{fast} \times C_{Al_2O_3,fast}(t) + k_{slow} \times C_{Al_2O_3,slow}(t)) - \frac{Fa(I_{line}(t))}{mass_{bath}} \quad (4)$$

where:

$C_{Al_2O_3,d}$	Concentration of dissolved alumina, %wt

$Fa(I_{line}(t))$ Alumina consumption rate based on the Faraday's Law which can be calculated by the following equation:

$$Fa(I_{line}(t)) = \frac{I_{line}(t) \times M_{Al_2O_3} \times CE(t)}{F \times z} \quad (5)$$

where:

I_{line} Line current of the cell, A
$M_{Al_2O_3}$ Molar mass of alumina, g/mol
CE Current efficiency of the electrolysis process
F Faraday constant, 96 485.3321 C/mol
z Number of transferred electrons = 3 for aluminium.

For the thermal balance modelling, line current flows through cells and provides energy for the process running. However, only the energy of 6.6 kWh/kg Al is utilised for aluminium production [14] and the rest is dissipated as heat. When calculating the heat in the bath, the external voltage drop does not contribute to heat generation. Taking into account heat transfer to the side, top and bottom, the bath temperature can be represented as follows:

$$\frac{dT_{bath}(t)}{dt} = \left(V_{cell}(t) - V_{ext}(t)\right) \times I_{line}(t) - 6.6 \times \frac{Fa(I_{line}(t))}{3600} - Q_{bathLedgesurf}(t) - Q_{bathAnode}(t) - Q_{bathCelltop}(t) - Q_{bathOtherBtm}(t) \quad (6)$$

where:

T_{bath}: Bath temperature of the cell, °C
V_{cell} Cell voltage, V
V_{ext} External voltage drop, V
$Q_{bathLedgesurf}$ Heat transferred from bath to the interface between bath and ledge, W
$Q_{bathAnode}$ Heat transferred from bath to the anode, W
$Q_{bathCelltop}$: Heat transferred from bath to the cell top space, W
$Q_{bathOtherBtm}$: Heat transferred from bath to the bottom of the cell, W.

The detailed calculating equations of these above heat related items can be found in [15] and the cell voltage equation proposed by Yao [16] is as follows:

$$V_{cell}(t) = h\left(I_{line}(t), ACD(t), C_{Al_2O_3,d}(t), \theta\right) \quad (7)$$

where:

ACD Anode-cathode distance, cm
θ Cell design and operating parameters.

In Equation (7), the function $h(\cdot)$ includes variable components that contribute to the cell voltage. These components include the reversible potential, the concentration overvoltage at anode, the surface overvoltage at anode, the concentration overvoltage at cathode, the ohmic resistance on anode, the ohmic resistance on bubble layer, the ohmic resistance on bath and the ohmic resistance on cathode. Each of these factors plays a role in determining the overall cell voltage.

3. Model Predictive Controller Design of the Aluminium Smelting Cell

The aluminium smelting process is highly nonlinear, the MPC can perform well in handling such nonlinear systems by incorporating process models. Based on the model, MPC can capture the complex behaviour and provide predictions. It can optimise control actions to achieve desired

setpoints while minimising the deviations from the reference trajectory, considering the future behaviour over a finite time horizon. On the other hand, MPC can explicitly incorporate constrains on variables, such as input limits and output limits, into the optimisation problem, ensuring these constrains are satisfied throughout the control horizon. This capability of MPC enables optimised control of the aluminium smelting process and improving overall process performance.

The discrete time form of the above system (Equations (2)-(6)) can be written as follows:

$$
\begin{aligned}
C_{Al_2O_3,fast}(k+1) &= C_{Al_2O_3,fast}(k) + t_s\left(-k_{fast} \times C_{Al_2O_3,fast}(k) + \frac{mass_{feed} \times r}{mass_{bath}}\right) \\
C_{Al_2O_3,slow}(k+1) &= C_{Al_2O_3,slow}(k) + t_s\left(-k_{slow} \times C_{Al_2O_3,fast}(k) + \frac{mass_{feed} \times (1-r)}{mass_{bath}}\right) \\
C_{Al_2O_3,d}(k+1) &= C_{Al_2O_3,d}(k) + t_s\left(k_{fast} \times C_{Al_2O_3,fast}(k) + k_{slow} \times C_{Al_2O_3,slow}(k) - \frac{Fa(I_{line}(k))}{mass_{bath}}\right) \\
T_{bath}(k+1) &= T_{bath}(k) + t_s\left(\left(V_{cell}(k) - V_{ext}(k)\right) \times I_{line} - 6.6 \times \frac{Fa(I_{line}(k))}{3600} - \right. \\
&\qquad \left. Q_{ledgesurfBath}(k) - Q_{bathAnode}(k) - Q_{bathCelltop}(k) - Q_{bathOtherBtm}(k)\right)
\end{aligned}
\tag{8}
$$

where:

k Index of discrete samples

t_s Sampling time, s.

To represent this model in a simple way, it can also be rewritten as follows:

$$
\begin{aligned}
x(k+1) &= f(x(k), u(k)) \\
y(k) &= Cx(k)
\end{aligned}
\tag{9}
$$

where:

system states $x(k) = \left[C_{Al_2O_3,fast}(k), C_{Al_2O_3,slow}(k), C_{Al_2O_3,d}(k), T_{bath}(k)\right]^T$

system output $y(k) = \left[C_{Al_2O_3,d}(k), T_{bath}(k)\right]^T$

control input of this system $u(k) = \left[mass_{feed}(k), ACD(k)\right]^T$

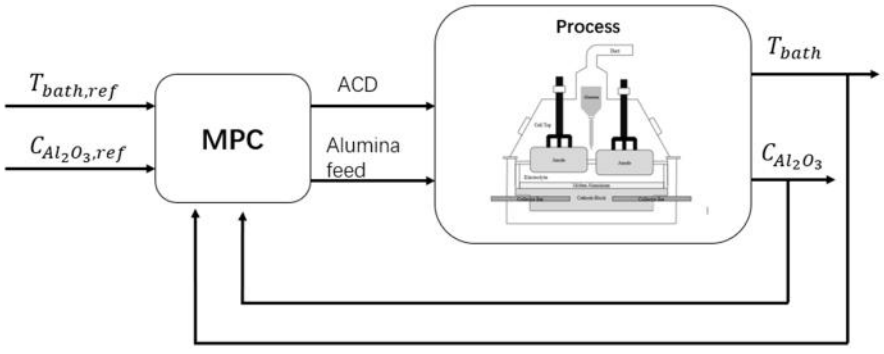

Figure 2. The control diagram for MPC.

Before implementing the control, the following assumptions need to be made:

- **Assumption 1:** With the use of soft sensors, it is assumed that the bath temperature and the alumina concentration can be estimated in real-time, using methodologies previously published in [4, 17].

- **Assumption 2:** It is assumed that the concentration of aluminium fluoride and other bath compositions are well controlled and remain relatively constant.

Under these assumptions, to achieve a stable superheat for the process, the control diagram is depicted in Figure 2, the control inputs are alumina feed and ACD and the controlled variables are alumina concentration and bath temperature.

To maintain stable process conditions, the target reference values for the bath temperature and alumina concentration can be set to facilitate a smooth transition between operating points. These reference values can be calculated by considering the relationships between superheat, bath temperature, and liquidus temperature. Under the above assumptions, the liquidus temperature can be determined based on the alumina concentration. By considering these interrelated factors, it becomes feasible to optimise the control inputs (alumina feed and ACD) and ensure a stable thermal balance throughout the process. The use of an MPC controller further facilitates this goal by driving the process towards the target reference values. The fluctuations in superheat during power modulation can be finally minimised, leading to improved stability of the process.

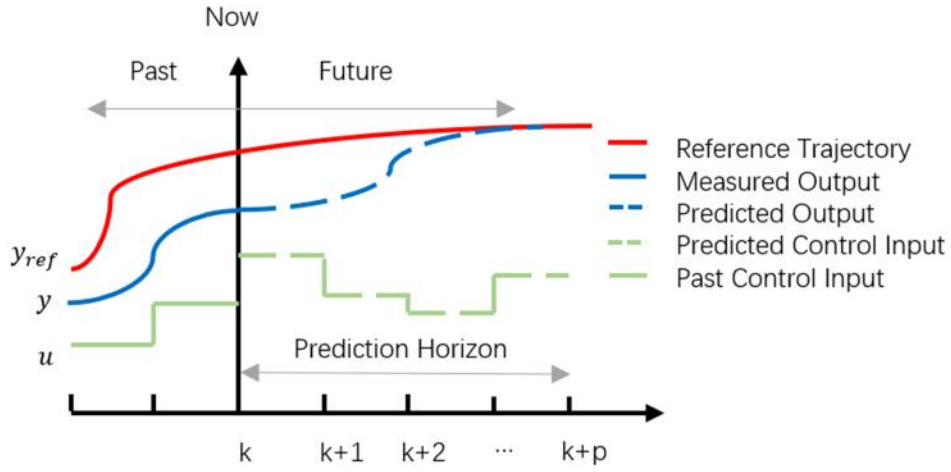

(a) The operation of MPC controller at the k time

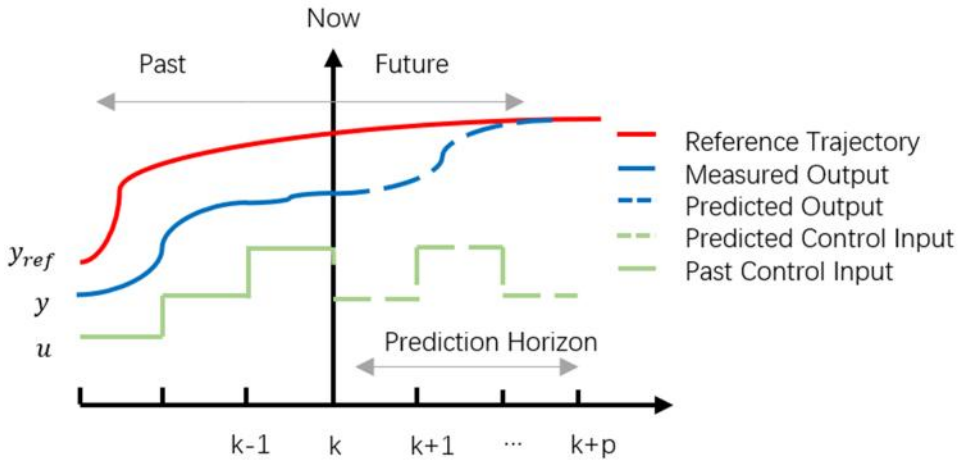

(b) The operation of MPC controller at the next time

Figure 3. The running mechanism of MPC.

To drive the alumina concentration and bath temperature towards the target reference values, this control problem can be described as follows:

$$\min J = \min \sum_{k=0}^{n} \left(\left(y(k) - y_{ref}\right)^T Q \left(y(k) - y_{ref}\right) + (\Delta u(k))^T R \Delta u(k) \right) \quad (10)$$

$$s.t \quad x(k+1) = f(x(k), u(k)), y(k) = Cx(k)$$
$$mass_{feed,min} \leq mass_{feed}(k) \leq mass_{feed,max}$$
$$ACD_{min} \leq ACD(k) \leq ACD_{max}$$
$$ACD(k+1) - ACD(k) \leq b$$

where the cost function is composed of two terms: the output error and the change rate of input, with weighting matrices Q and R. The second term, which is related to Δu, is included to prevent large beam movements. The system output y (alumina concentration and bath temperature), and state variables x, are subject to the system dynamics $f(\cdot)$ as defined in Equation (9). The alumina feed is constrained by the lower bound $mass_{feed,min}$ and upper bound $mass_{feed,max}$ respectively. Similarly, the minimum and maximum anode-cathode distance are considered through ACD_{min} and ACD_{max}. Furthermore, the maximum allowed movement of anode beam between two sampling times is also limited by b.

When using MPC to address this problem, the detailed steps are illustrated in Figure 3. Firstly, the target trajectory for the bath temperature and alumina concentration is set. Then the controller calculates the optimal process control input based on the cost function within the prediction horizon. These control inputs will drive the process variables to the target reference values, as shown in Figure 3 (a). Subsequently, only the first predicted control input is applied to the process, and at the next time step, the controller recalculates a new control input within the prediction horizon, as shown in Figure 3 (b). Then the controller constantly repeats these steps to achieve the control of the target variables.

4. Simulation Results

To test the effectiveness of this method, two scenarios are considered in this section. The parameters in this simulation are set as: $mass_{feed,min}$ =50 g , $mass_{feed,max}$ =200 g, ACD_{min}=2.3 cm, ACD_{min}=3.3 cm, $Q = diag(1,1)$ and $R = diag(0,0.01)$.

4.1 Case 1: Increase the Line Current

In this case, the line current is increased by 5% from the 1st hour to the 3rd hour, as shown in Figure 4, and the system performance of other variables under MPC is also shown below.

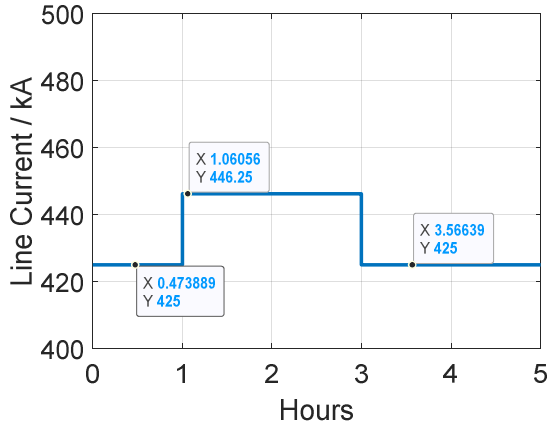

Figure 4. Line current change of the process operation.

Figure 5 (a) illustrates the successful achievement of stable superheat throughout the entire simulation period, with the superheat maintained at approximately 12 °C. Figure 5 (b) demonstrates the response of the ledge thickness under MPC, it shows that the variation in ledge thickness during the 5 % line current modulation, when compared to the situation without MPC, is less than 1 cm. In the scenario without MPC, only the line current is increased without any ACD change and alumina concentration alteration. The reason for the ledge thickness not returning to its original value is that the equilibrium point has shifted due to the increase in line current. This increase in energy input to the cell results in the ledge becoming thinner to maintain the new thermal balance. In Figure 6, the control inputs utilised during power modulation under the MPC control method are presented. The alumina feed and ACD are adjusted to meet the target value, ensuring that the desired alumina concentration is maintained. When the line current increases, the alumina feed rate is decreased to attain the desired reduced alumina concentration. Once this concentration is achieved, during the period of 1.6-3 hours, the alumina feed rate is subsequently increased to meet the rising alumina demand caused by the increase in line current. Figure 7 demonstrates that both the bath temperature and the alumina concentration can reach the target reference values under the application of MPC. Based on Figure 6 and Figure 7, there are observed overshoots in the alumina feed and ACD. These overshoots occur at the same time as the turning points of the alumina concentration and bath temperature. The reason for these overshoots can be attributed to the insufficient prediction horizon used in the MPC controller for computer performance reasons.

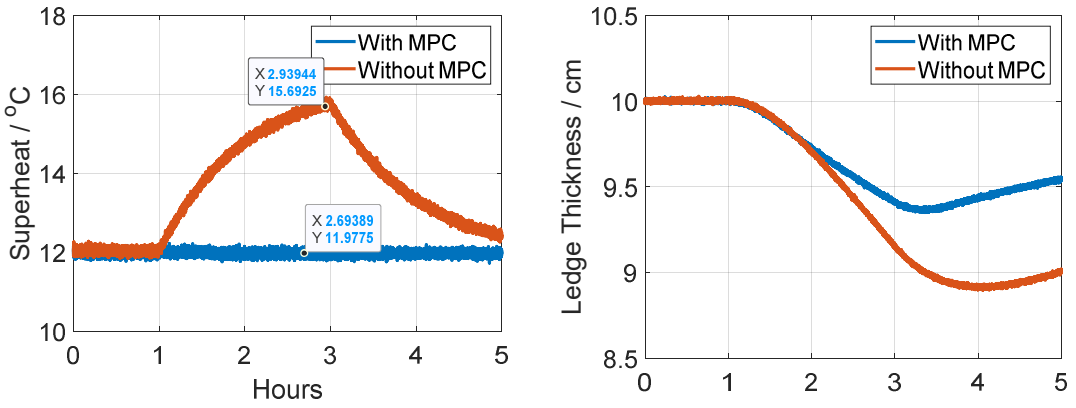

(a) Superheat (b) Ledge thickness

Figure 5. Response of superheat and ledge thickness with and without MPC (line current increased by 5 % at 1 h and returned at 3 h).

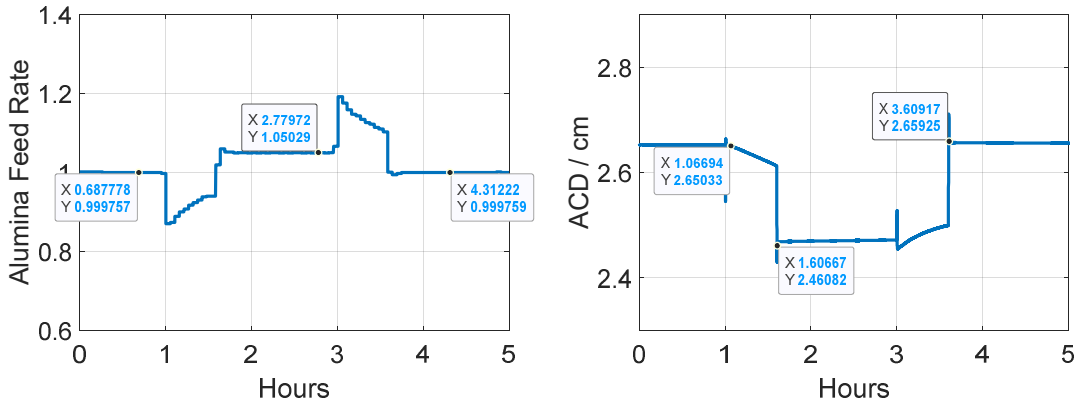

(a) Alumina feed under MPC (b) ACD under MPC

Figure 6. Control inputs of the MPC controller (line current increased by 5 % at 1 h and returned at 3 h).

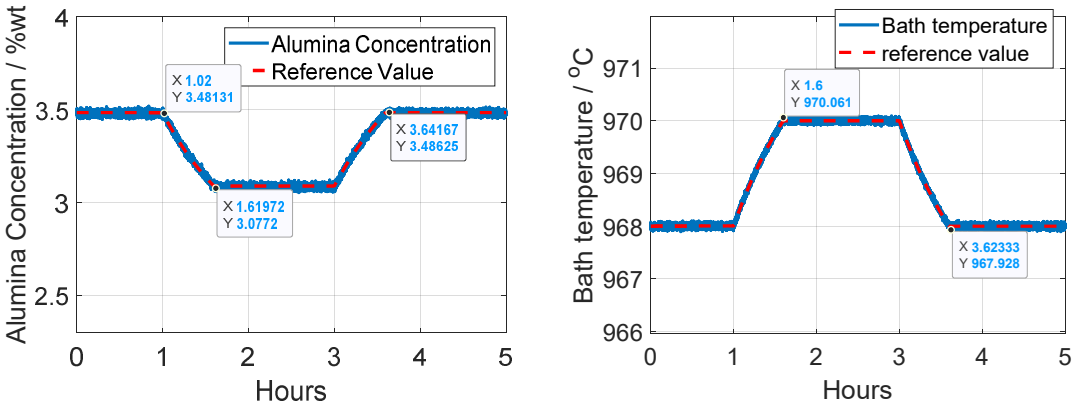

(a) Response of alumina concentration (b) Response of bath temperature

Figure 7. System outputs under MPC control (line current increased by 5 % at 1 h and returned at 3 h).

4.2 Case 2: Decrease the Line Current

In this case, the line current is decreased by 5 % from the 1st hour to the 3rd hour, as shown in Figure 8, and the system performance of other variables under MPC is shown below.

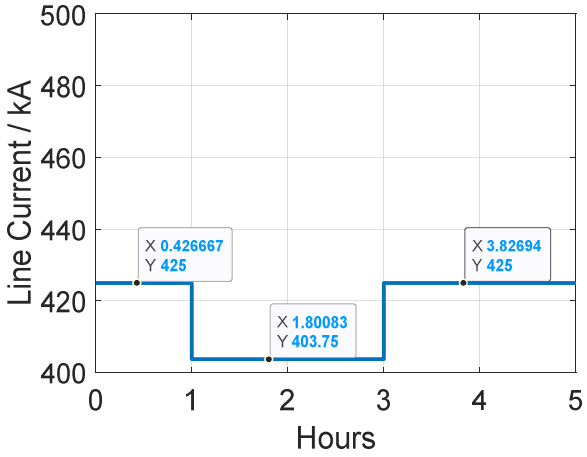

Figure 8. Line current change of the process operation.

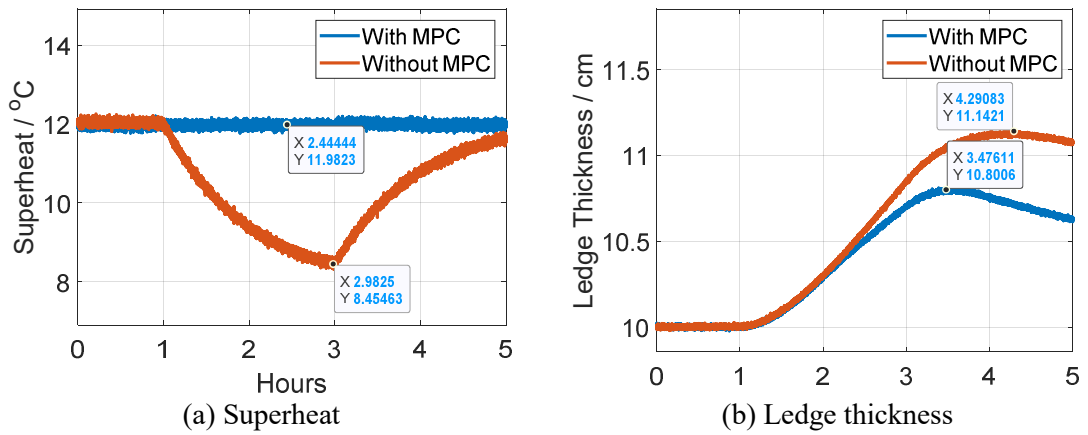

(a) Superheat (b) Ledge thickness

Figure 9. Response of superheat and ledge thickness with and without MPC (line current decreased by 5 % at 1 h and returned at 3 h).

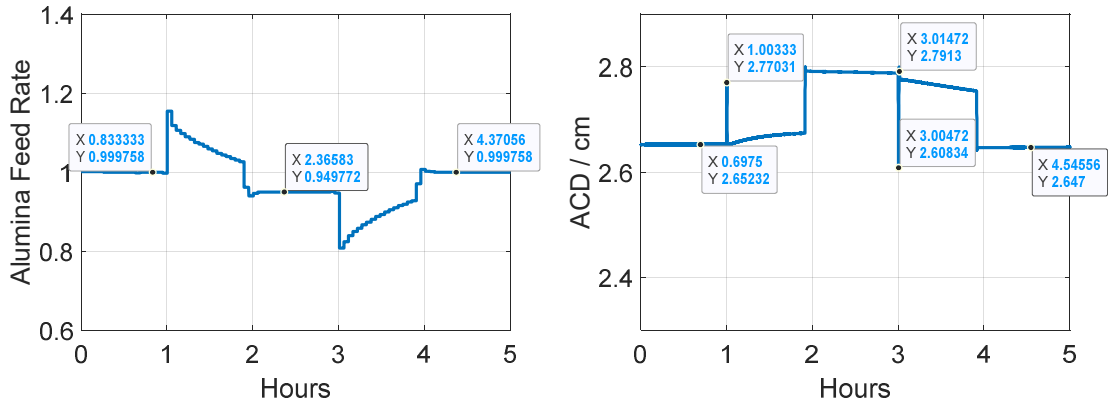

(a) Alumina feed under MPC (b) ACD under MPC

Figure 10. Control inputs of the MPC controller (line current decreased by 5 % at 1 h and returned at 3 h).

Similar to the behaviour observed when the line current is increased, the superheat remains within a certain range as the line current drops, as depicted in Figure 9 (a). Figure 9 (b) illustrates that the variation of the ledge thickness during the 5 % line current decrease is less than 1 cm, in contrast to the situation without MPC. Similarly, in the absence of MPC, the scenario involves solely decreasing the line current without making any adjustments to the ACD and alumina concentration. The ledge thickness does not return to its original value due to the reduced energy input to the cell. This decrease in energy causes the ledge to become thicker, as it adjusts to maintain the new thermal balance. Figure 10 and Figure 11 present the control inputs employed and corresponding response of bath temperature and alumina concentration. Once the desired alumina concentration remains constant, the alumina feed can be maintained at a constant level. The overshoots (approximately 0.1 cm) observed in the ACD control can also be attributed to the insufficient prediction horizon employed in the MPC controller for computer performance reasons.

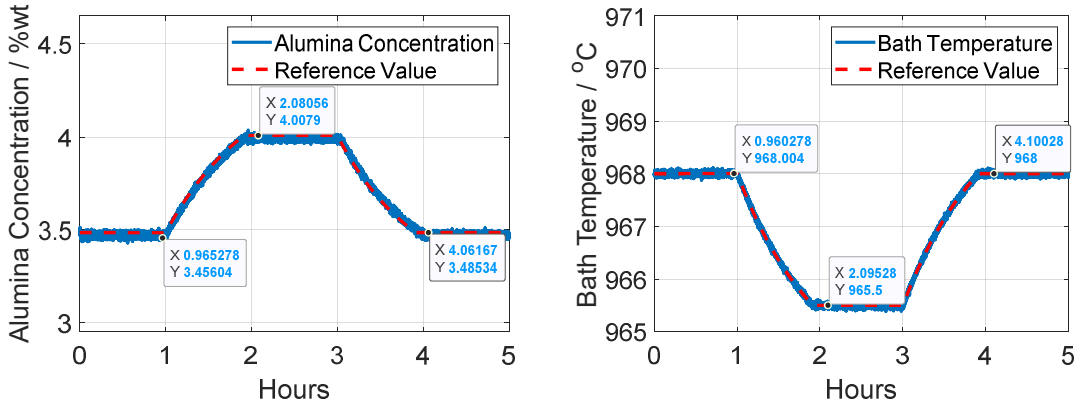

(a) Response of alumina concentration (b) Response of bath temperature

Figure 11. System outputs under MPC control (line current decreased by 5 % at 1 h and returned at 3 h).

5. Conclusions

Superheat plays a critical role in the aluminium smelting process as it impacts energy consumption and cell lifespan. Maintaining stable superheat is vital for efficient operation. In this paper, the MPC method is employed to maintain a stable superheat by manipulating the alumina feed and ACD, driving the process variables of alumina concentration and bath temperature towards their reference values. By optimizing these variables while considering constraints with MPC, the paper demonstrates stable superheat performance during power modulation. This research lays a foundation for enhancing process performance during power modulation. In future research studies, it would be beneficial to improve the accuracy of the model and explore more advanced control strategies to overcome limitations and further advance the application of MPC.

6. References

1. Peter M. Entner. Control of bath temperature, *Essential Readings in Light Metals: Volume 2 Aluminum Reduction Technology*, 2016, 808-811, from *Light Metals* 1995, 227-232.
2. Tormod Drengstig, *On process model representation and AlF_3 dynamics of aluminium electrolysis cells,* Dr Ing Thesis, Department of Engineering Cybernetics, Norwegian University of Science and Technology (NTNU), Trondheim, Norway, August 1997.
3. S, Kolås, and T. Støre, Bath temperature and AlF_3 control of an aluminium electrolysis cell. *Control Engineering Practice* 17 9 2009, 1035-1043.
4. Jing Shi, *Advanced alumina feeding control of aluminium smelting cell*, PhD Thesis, UNSW, Sydney, 2021.
5. Shuiping Zeng, Shasha Wang and Yaxing Qu, Control of temperature and aluminum fluoride concentration based on model prediction in aluminum electrolysis, *Advances in materials science and engineering* 2014, https://doi.org/10.1155/2014/181905.
6. Y. X. Liu and Jie Li, *Modern aluminum electrolysis*, Metallurgy Industry Publication, Beijing, China 90, 2008.
7. Yuchen Yao, *Process monitoring, modelling and fault diagnosis in aluminium reduction cells*, PhD Thesis, UNSW, Sydney, 2017.
8. Tormod Drengstig, Dag Ljungquist and Bjarne A. Foss, On the AlF_3 and temperature control of an aluminium electrolysis cell, *Modelling, Identification and Control* 1998, vol 19, No 1, 31-59.
9. Richard G. Haverkamp and Barry J. Welch, Modelling the dissolution of alumina powder in cryolite, *Chemical Engineering and Processing: Process Intensification* 37 2, 1998, 177-187.
10. Marc Dupuis, Modeling power modulation, *Light Metals* 2002. 489-494.
11. David Eisma and Pretesh Patel, Challenges in power modulation." *Essential Readings in Light Metals: Volume 2 Aluminum Reduction Technology* 2016, 683-688, original in Light Metals 2009, 327-332.
12. Biedler Philip, *Modeling of an aluminum reduction cell for the development of a state estimator*, PhD Thesis, West Virginia University, 2003.
13. Jing Shi, *Advanced alumina feeding control of aluminium smelting cell*, PhD Thesis, UNSW, Sydney, 2021.
14. Barry J. Welch, Specific energy consumption and energy balance of aluminium reduction cell, Presentation at *8th international congress "Non-ferrous Metals & Minerals"*, Krasnoyarsk, Russia, 2016.
15. Choon-Jie Wong et al, Discretized thermal model of Hall-Héroult cells for monitoring and control, *IFAC-Papers Online* 54, 11 2021, 67-72.
16. Yuchen Yao et al, Estimation of spatial alumina concentration in an aluminum reduction cell using a multilevel state observer, *AIChE Journal* 63 7, 2017, 2806-2818.

Fabio Soares, Limao Roberto and Castro Marcos, Bath temperature inference through soft sensors using neural networks, *Light Metals* 2010, 467-472.